Multi-functional graphene/leather for versatile wearable electronics

Qiaohang Guo[1, *], Jing Guo[1], Huamin Chen[2, *], Peidi Zhou[3], Congwei Li[1], Kaihuai Yang[4], Nengbin Hua[1], Jun Wang[2], Mingcen Weng[1, *]

1 School of Materials Science and Engineering, Fujian Provincial Key Laboratory of Advanced Materials Processing and Application, Key Laboratory of Polymer Materials and Products of Universities in Fujian, Fujian University of Technology, Fuzhou, Fujian 350118, China

2 Fujian Key Laboratory of Functional Marine Sensing Materials, College of Materials and Chemical Engineering, Minjiang University, Fuzhou 350108, China

3 Institute of Smart Marine and Engineering, Fujian University of Technology, Fuzhou, Fujian, 350118, China
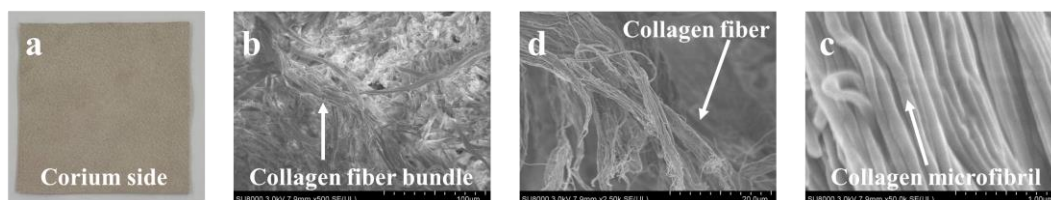
4 School of Mechanical and Intelligent Manufacturing, Fujian Chuanzheng Communications College, Fuzhou, Fujian 350007, China
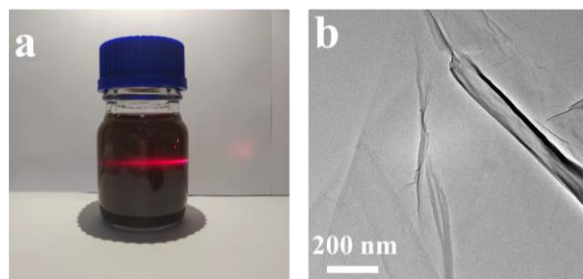
* Corresponding author:

Qiaohang Guo, guoqh@fjut.edu.cn

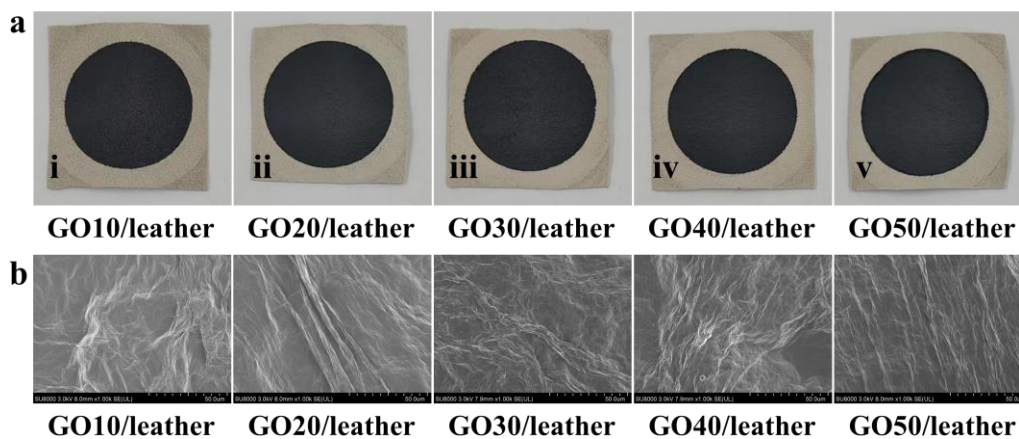Huamin Chen, chenhuamin@mju.edu.cn
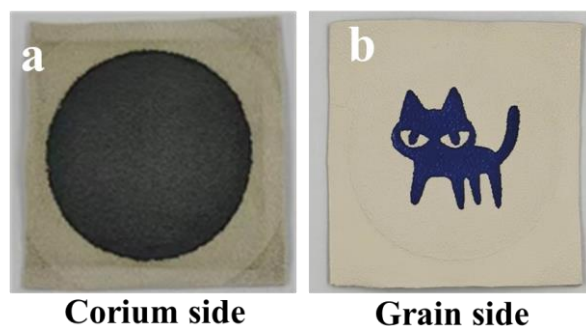
Mingcen Weng, wengmc@fjut.edu.cn

Fig. S1. The hierarchical structure of the leather. (a) Leather. (b) Collagen fiber bundle.

(c) Collagen fiber. (d) Collagen microfibril.

Fig. S2. (a) GO dispersion (0.1 mg mL^{-1}). (b) TEM image of GO sheets.

Fig. S3. Optical photos (a) and SEM images (b) of GO/leathers.

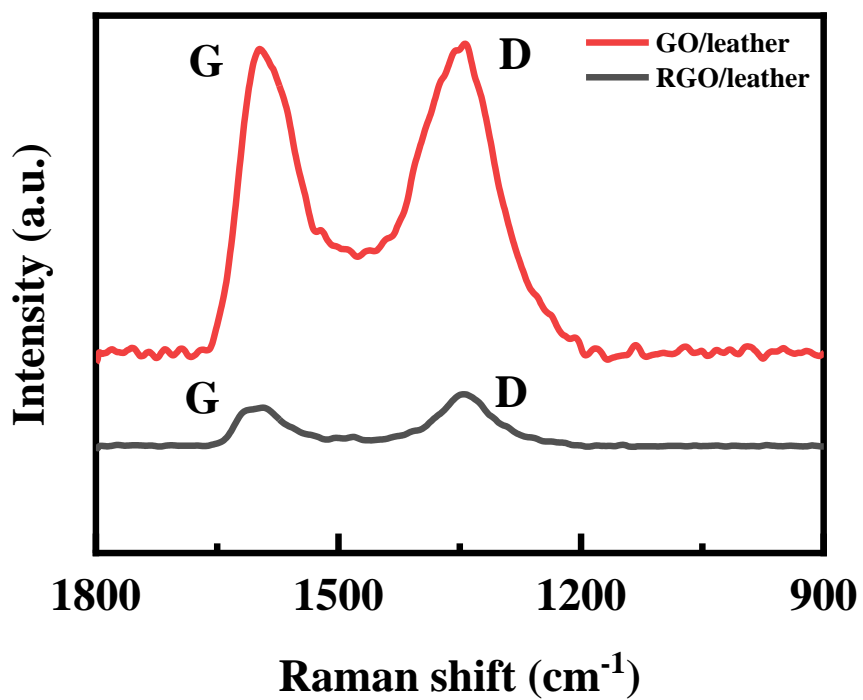**Fig. S4.** Optical photos of the multi-functional RGO50/leather.

Fig. S5. Raman spectra of GO/leather and RGO/leather.
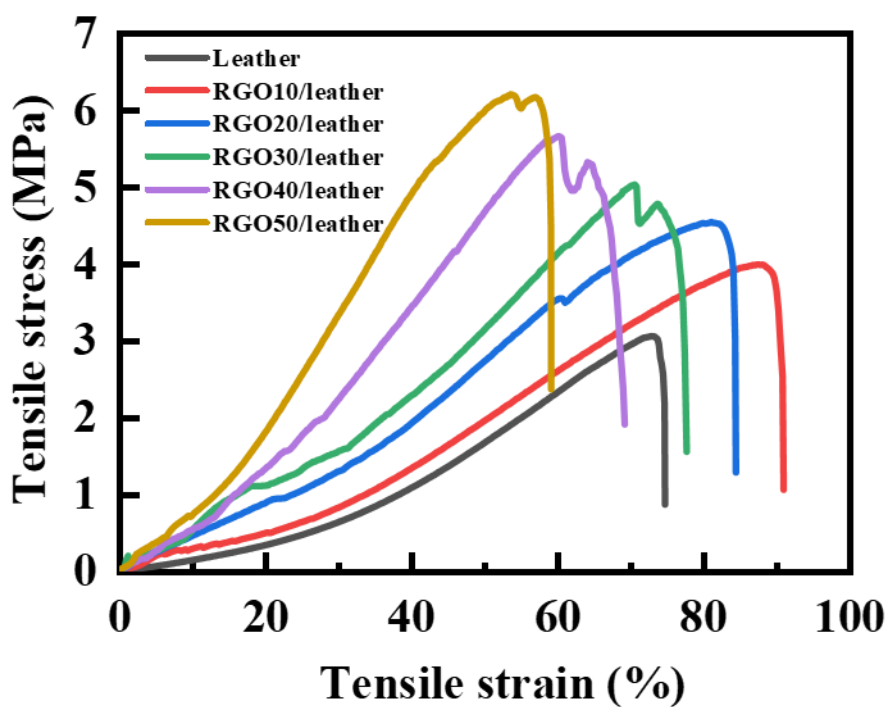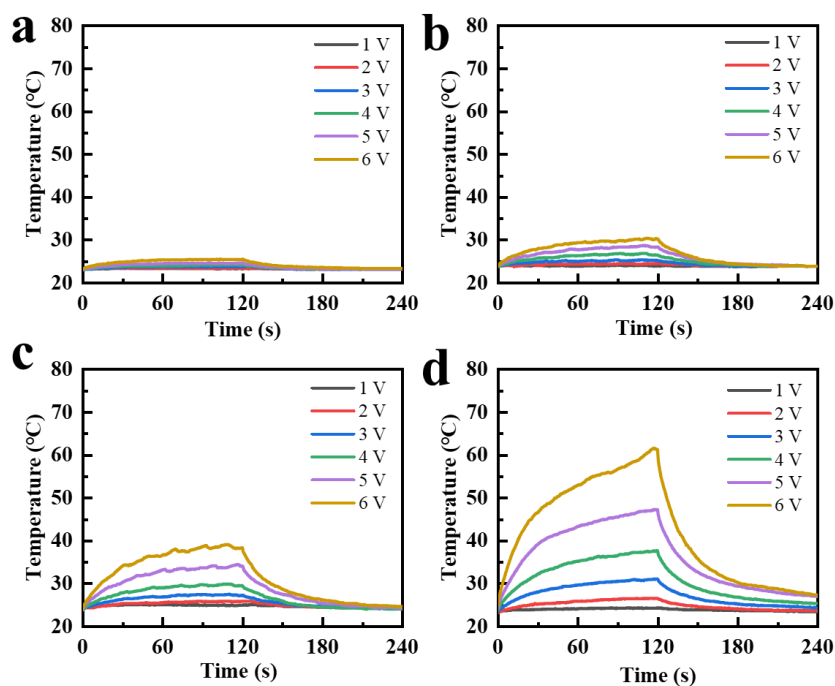

Fig. S6. Tensile stress-strain curves of leather and RGO/leathers.

Fig. S7. The surface temperature of the RGO10/leather (a), RGO10/leather (b), RGO10/leather (c), and RGO10/leather (d) with different driven voltages.
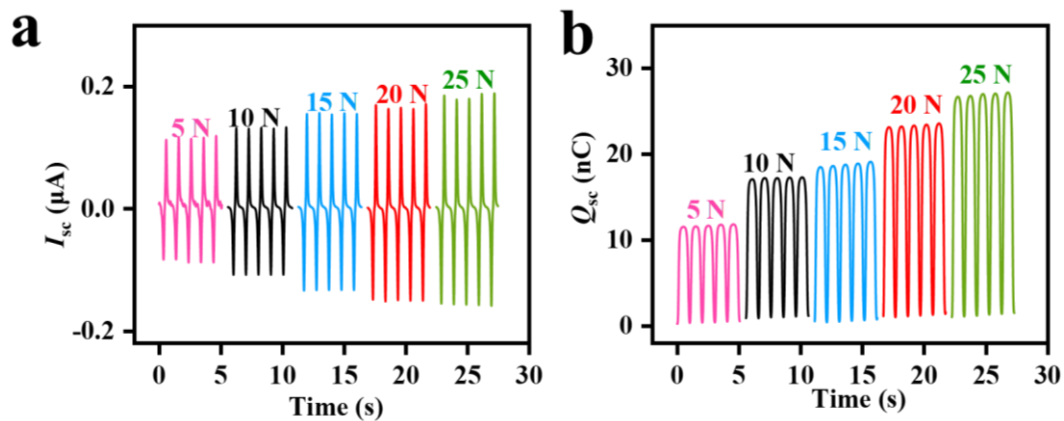
Fig. S8. Short-circuit current (a), and transferred charge (b) of RGO/leather TENG.

under different loading pressure between 5-25 N.
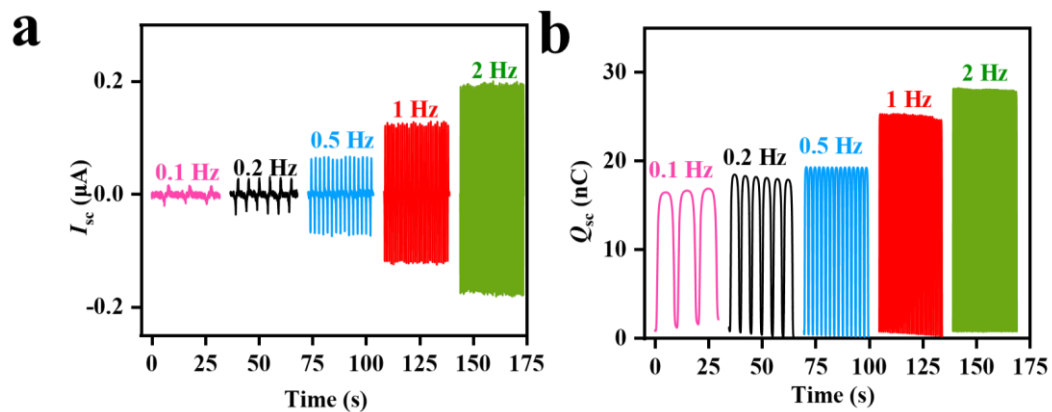
Fig. S9. Short-circuit current (a), and transferred charge (b) of RGO/leather TENG. under different loading frequencies between 0.1 and 2 Hz.
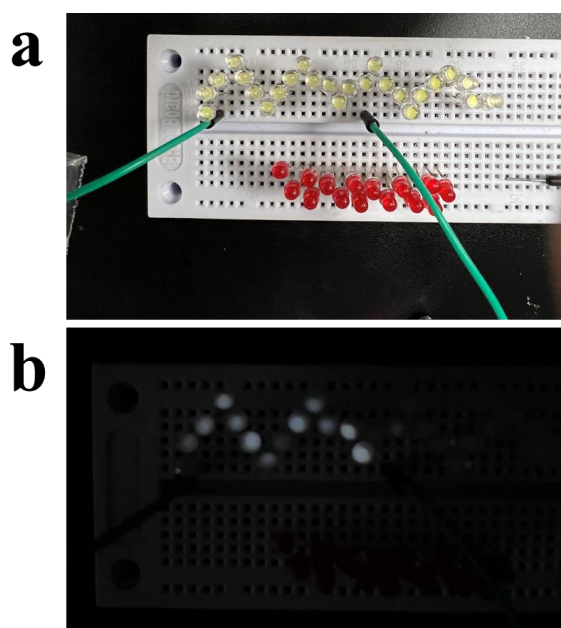
Fig. S10. The photograph of a self-powered display system driven by RGO/leather TENG.

Initial state　　　　　　　　**After 12 h**

Fig. S11. The gel electrode and leather electrode were covered on the arm for 12 h and then removed from the arm. The skin under the gel electrode became greasy, while the skin under the leather electrode is changed.
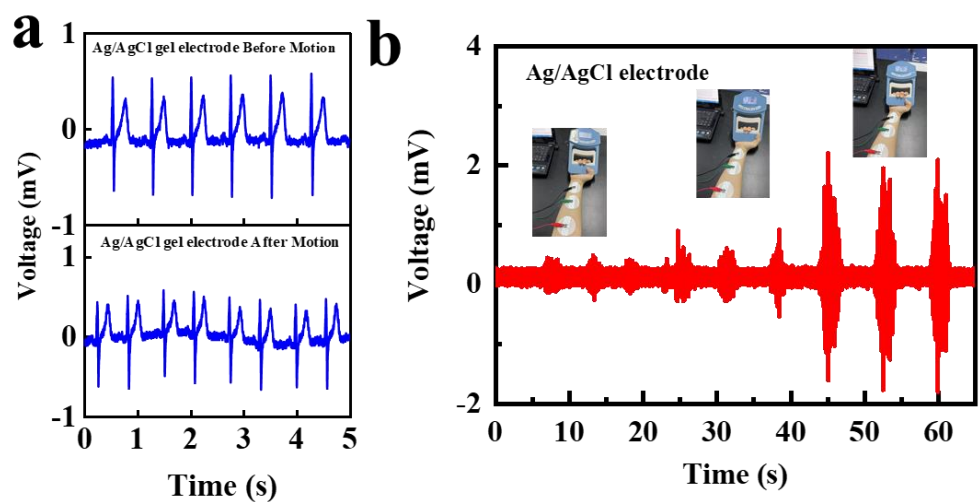
Fig. S12. The ECG signals of a volunteer were collected from Ag/AgCl gel electrodes (a). The EMG signals of a volunteer were collected from Ag/AgCl gel electrodes (b).
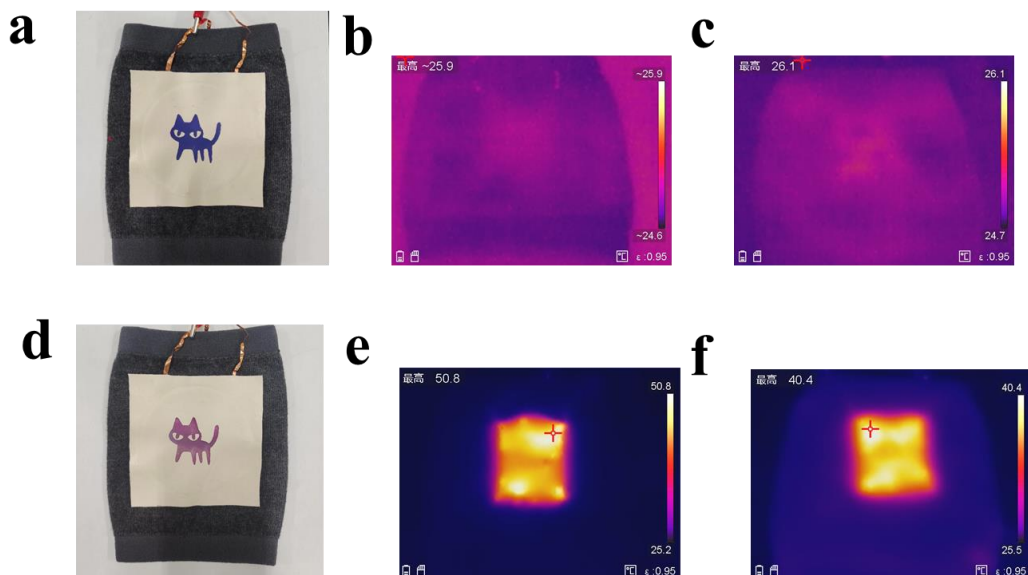
Fig. S13. (a) Optical photo of the initial state of the smart kneepad. The infrared images of the external (b) and internal (c) temperature of the initial state of the kneepad. (d) Optical photo of the heating state of the smart kneepad. The infrared images of the external (e) and internal (f) temperature of the heating state of the kneepad.
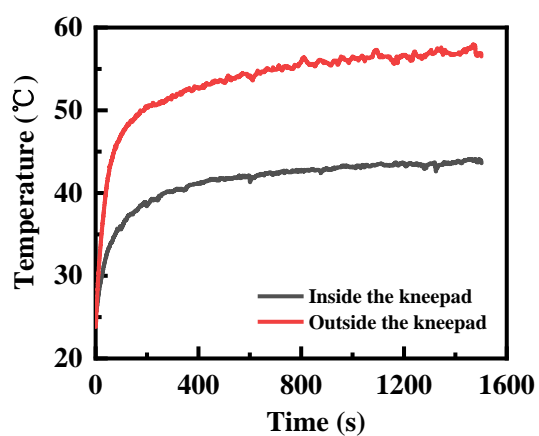
Fig. S14. Thermal stability of the smart kneepad made with RGO50/leather with a driven voltage of 5 V.
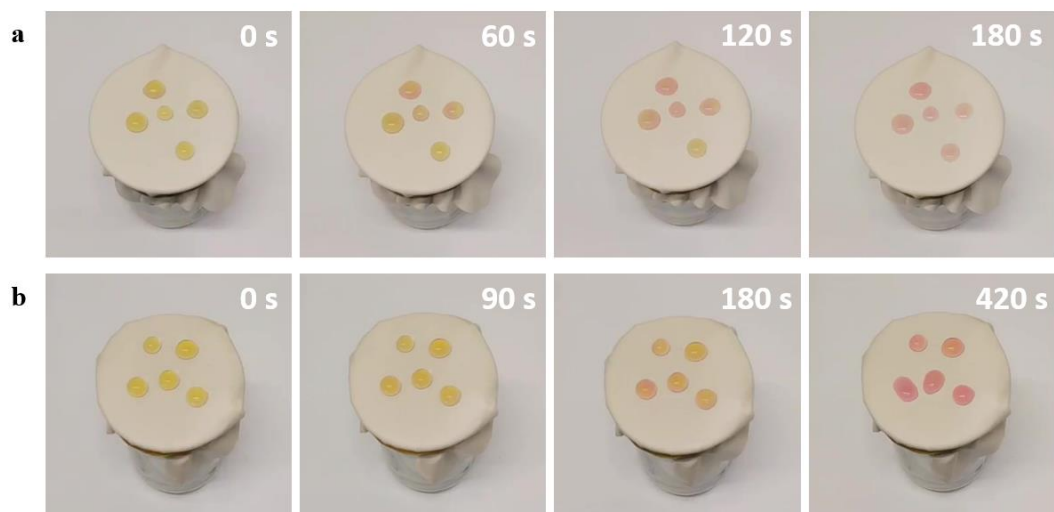
Fig. S15 The air permeability test of (a) pure leather, and (b) RGO50/leather. To demonstrate the air permeability of RGO/leather, pure leather, and RGO50/leather are covered on a beaker containing 20 mL of HCl. Methyl orange droplets on the surface of the pure leather and RGO50/leather are used as an indicator. The color change time of the methyl orange droplets on the surface of the RGO50/leather (420 s) is slightly longer than that of the pure leather (180 s).
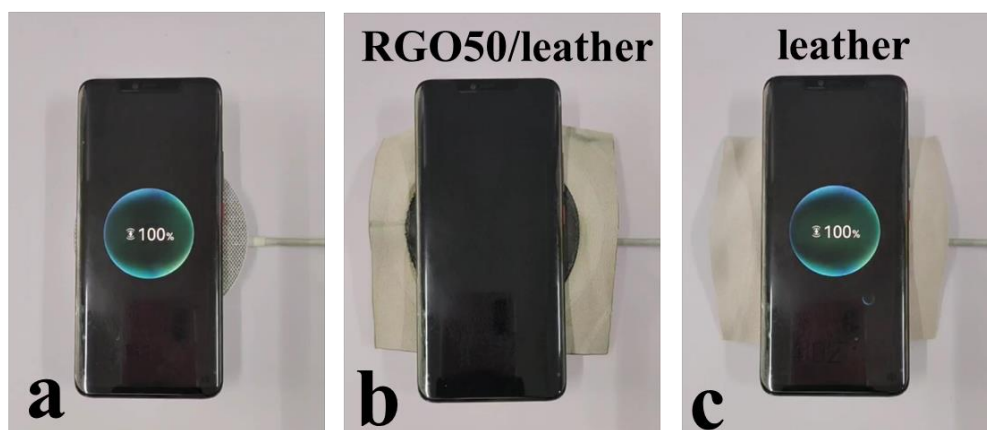
Fig. S16. The photos show the EMI shielding effect of the RGO50/leather between a wireless charger and a smartphone.
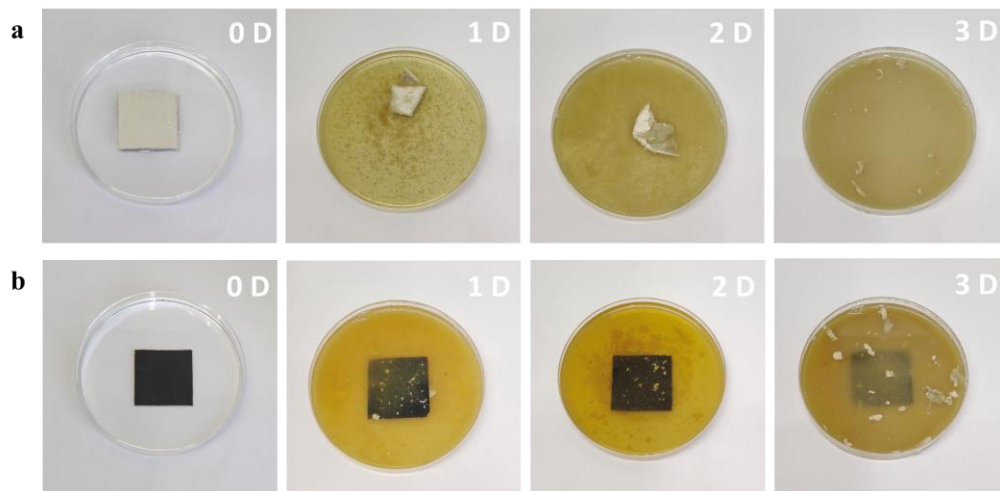
Fig. 17. Biodegradability of (a) leather, and (b) RGO50/leather. the pure leather and RGO50/leather with dimensions of 3 cm × 3 cm are immersed in 20 mL of alkaline protease solution with pH=10. During the process of biodegradation, the pure leather completely degrades within 3 days, as shown in Fig. 17(a). In contrast, the RGO layer of the RGO50/leather does not change significantly within 3 days, while the leather layer is completely degraded (Fig. 17(b)).

Table S1 Comparison of flexible electronics based on leather

Sample Name	Thermal management devices	TENGs	Flexible sensors	EMI shielding devices	Physiological sensors	Reference
RGO/leather	✓	✓		✓	✓	**This work**
LM-Cu@Ag				✓		J. Mater. Chem. C.2016, 4, 914-920
a-CNTs/Leather			✓			Adv. Sci. 2018,1801283
AgNWs/leather					✓	ACS Appl. Bio Mater. 2019, 2, 4, 1427−1431
CB/leather			✓			Adv. Mater. Technol. 2019, 4, 1900442
AgNWs /leather			✓			J Leather Sci. Eng. 2019, 1, 7
LDW carbonized leather (LDW-CL)			✓			Adv. Electron. Mater. 2020, 2000549
PPy-Leather					✓	Adv. Electron. Mater. 2020, 2000259
CB/leather			✓			J. Mater. Chem. C. 2020,8, 9748-9754
SWCNT/leather			✓			Macromol. Mater. Eng. 2020, 2000181
a-CNTs@leather			✓			Sci. China Technol. Sci. 2020, 63, 2137−2146
Ag/leather					✓	Biosensors. 2021, 11, 101
Ag/leather					✓	J Mater Sci: Mater Electron.2021, 32:4891–4902
AgNWs/leather	✓		✓	✓		Angew. Chem. Int. Ed. 2022, e202200705
PCBDA@AgNPs-CFN			✓			ACS Appl. Mater. Interfaces 2022, 14, 21645−21656
graphene/leather			✓			*J. Clean. Prod.* 2022,133360,371
PPy/SCB@PP-CFs	✓		✓			J. Mater. Chem. A, 2023,11, 726-741

Note S1. Thermodynamic analysis of the RGO/leather

When applying a certain voltage to the RGO/leather, an electrical current will pass through the RGO/leather, thus achieving the Joule heating process of electric-thermal conversion. Based on Joule's law, the heating performance of RGO/leather can be defined as follows:

$$P_{in} = UI \tag{1}$$

where P refers to the electrical power and resistance of RGO/leather, U refers to the driven voltage, and I refers to the circulating current.

According to the law of conservation of energy, the heat converted by the electric heating layer (Joule heat) should be equal to the sum of the total heat storage of the RGO/leather and the heat exchange with the environment. Thus, ignoring the conduction losses of the thermal management system, the energy balance relationship can be described as follows:

$$P_{in} = UI = P_{out} = Cm\frac{dT(t)}{dt} + Ah(T(t) - T_0) + \sigma A\varepsilon(T(t)^4 - T_0{}^4) \tag{2}$$

where m refers to the mass, C refers to the specific heat capacity, A refers to the surface area, h refers to the convective heat transfer coefficient, $T(t)$ refers to the instantaneous temperature of RGO/leather, T_0 refers to the initial temperature of the environment, σ refers to the Stefan-Boltzmann constant, and ε refers to the emissivity. The first term on the right represents the whole heat value that is responsible for the temperature elevation of the RGO/leather. The second term stands for heat loss by convection (h and A are the convective heat-transfer coefficient and the area of the RGO/leather, respectively). In addition, the third term is the heat loss of radiation (σ and ε are the Stefan-Boltzmann constant and the emissivity of the RGO/leather, respectively).

According to the previous report [S1], the basic strategy for quantifying the efficiency of conversion from electrical to thermal power is to record the surface temperature of the RGO/leather, the driven voltage, and the circulating current. First, we fabricated RGO/leather with different RGO contents as described in Experimental Section. Second, driven by a driven voltage for 120 s, the temperature of RGO/leather

reached a maximum and steady value. Therefore, at the steady state ($\frac{dT(t)}{dt} = 0$), the input thermal energy (converted from electrical power) is approximated equal to heat dissipation power:

$$UI = Ah(T_{max} - T_0) + \sigma A\varepsilon(T_{max}^4 - T_0^4). \tag{3}$$

According to the previous report, considering the low-temperature ranges, equation (2) can be linearized by neglecting the nonlinear term of the radiation loss [S2]. Thus, equation (3) can be modified as:

$$UI = Ah(T_{max} - T_0). \tag{4}$$

Therefore, the electric-thermal conversion efficiency of the RGO/leather η and T_{max} can be calculated as follows:

$$\eta = \frac{P_{out}}{P_{in}} = \frac{Ah(T_{max} - T_0)}{UI}, \tag{5}$$

$$T_{max} = \frac{UI}{Ah} + T_0 = \frac{U^2}{AhR} + T_0, \tag{6}$$

where, $A = 6.76\ cm^2$, $h = 25\ W\ m^{-2}\ K^{-1}$, $\sigma = 5.67 \times 10^{-8}\ W\ m^{-2}\ K^{-4}$, $\varepsilon = 0.95$.

Table S2 Electric-thermal conversion efficiency of the RGO/leather

Sample	RGO10/leather	RGO20/leather	RGO30/leather	RGO40/leather	RGO50/leather
P_{in}/W	0.048	0.064	0.036	0.102	0.031
T_{max}/°C	25.6	26.9	25.0	28.1	24.6
T_0/°C	23.2	23.9	23.2	23.1	23.1
η/%	85	80	85	83	82

Note S2. Evaluation principle and comparison of EIM shielding properties

According to the Schelkunoffs theory, the total EMI shielding effectiveness (SE_T) consists of the reflection (SE_R), absorption (SE_A), and multiple reflections (SE_M), where the SE_M value can be ignored when the SE_T is above 10 dB. Thus, it can be expressed as:

$$SE_T = SE_A + SE_R, \tag{7}$$

To calculate SE_T, SE_A, and SE_R values, the power coefficients of reflection (R), absorption (A), and transmission (T) are determined based on the S_{11} and S_{21} parameters measured by the vector network analyzer as follows:

$$R = |S_{11}|^2, \tag{8}$$

$$T = |S_{21}|^2, \tag{9}$$

$$A = 1 - R - T, \tag{10}$$

$$SE_R = -10\log(1 - R), \tag{11}$$

$$SE_A = -10\log\left(\frac{T}{1-R}\right), \tag{12}$$

$$\text{Shielding efficiency} = 100 \times \left(1 - \frac{1}{10^{\frac{SE_T}{10}}}\right). \tag{13}$$

Reference

S1. Weng, M., Zhou, P., Chen, L., Zhang, L., Zhang, W., Huang, Z., Liu, C. and Fan, S., Adv. Funct. Mater., 2016, 26, 7244-7253.

S2. Liu, Q., Tian, B., Liang, J. and Wu, W., Materials Horizons, 2021, 8, 1634-1656.